Tellus
SERIES A
DYNAMIC
METEOROLOGY
AND OCEANOGRAPHY
PUBLISHED BY THE INTERNATIONAL METEOROLOGICAL INSTITUTE IN STOCKHOLM

Tellus (2011), 63A, 256–262
Printed in Singapore. All rights reserved

TELLUS

An evaluation study of the DRP-4-DVar approach with the Lorenz-96 model

By JUANJUAN LIU[1], BIN WANG[1]* and QINGNONG XIAO[2], [1]*LASG, Institute of Atmospheric Physics, Beijing 100029, China* [2]*College of Marine Science, University of South Florida, St. Petersburg, FL 33701, USA*

(Manuscript received 12 November 2009; in final form 30 August 2010)

ABSTRACT

The study evaluates the performance of the dimension-reduced projection four-dimensional variational data assimilation (DRP-4-DVar) with the Lorenz-96 model. Idealized experiments over a period of 200 days have been conducted. The results show that the DRP-4-DVar works well. It generates an analysis equivalent to that of the Ensemble Kalman Filter (EnKF) if the synchronous observations are assimilated at the analysis time, while it produces more accurate analysis than the EnKF does when assimilating observations in an 18-h assimilation window. The experiments also reveal that the impact of the tangent linear assumption for the Lorenz-96 model in the DRP-4-DVar over a 24-h or shorter assimilation window is negligible. Furthermore, with a background error covariance matrix (**B**-matrix) that has a non-singular projection onto the ensemble space or is explicitly flow-dependent, the DRP-4-DVar performs even better than with a **B**-matrix that has a singular projection or is not explicitly flow-dependent.

1. Introduction

Four-dimensional variational data assimilation (4-DVar, e.g. Le Dimet and Talagrand, 1986; Courtier and Talagrand, 1987; Courtier et al., 1994; Zou and Kuo, 1996; Wang et al., 2000; Xiao et al., 2000) has currently been adopted by five operational Numerical Weather Prediction (NWP) centres for global analysis (Rabier et al., 2000; Rawlins et al., 2007). However, its applications are still limited by the computer resources and the computational cost of its operational uses is expensive. In recent years, the NWP users give more and more attentions to the Ensemble Kalman Filter (EnKF; Evensen, 1994; Houtekamer and Mitchell, 1998, 2001), which requires less original investment in terms of coding. But EnKF is naturally designed to incorporate sequential information. Later, Hunt et al. (2004) extend EnKF to accurately assimilate asynchronous observations at the correct time. With a growing number of various asynchronous observations, it is necessary to explore more efficient assimilation techniques, which would overcome the disadvantages of 4-DVar and EnKF. Hybrid of 4-DVar and EnKF has therefore been proposed in the literature (e.g. Lorenc, 2003; Liu et al., 2008; Wang et al., 2010; Zhang et al., 2009).

Lorenc (2003) compared the potential of EnKF with 4-DVar in operational NWP assimilation systems and discussed the hybrid scheme. He noted that the hybrid scheme is attractive for limited-area mesoscale NWP systems. Kalnay et al. (2007a,b) also provided more detailed discussions of the pros and cons of EnKF and 4-DVAR. Gustafsson (2007) discussed the '4-DVar or EnKF' and concluded that the optimal approach is to combine the best ideas of both. Caya et al. (2005) directly compared EnKF with 4-DVar for storm-scale data assimilation and clearly demonstrated the strengths and weaknesses of each technique. Yang et al. (2009) compared variational and ensemble-based data assimilation schemes based on the quality of their analyses as well as their computational costs. Hamill and Snyder (2000) proposed a hybrid EnKF 3-DVar analysis scheme, which incorporates flow-dependent ensemble-estimated background error covariances into 3-DVar framework. Wang et al. (2007) described the theoretical equivalence of differently proposed ensemble-3-DVar hybrid analysis schemes. Evensen and Van Leeuwen (2000) extended EnKF to assimilate asynchronous observations (ensemble Kalman smoother). As extension to previously works, some new data assimilation approaches have been proposed gradually. The idea is to provide flow-dependent background error covariance matrices (simply **B**-matrices, hereinafter) of EnKF to 4-DVar with no extra computational cost (Buehner, 2005). Hunt et al. (2004) and Fertig et al. (2007) unified the EnKF and 4-DVar approach to introduce a 4-DEnKF. Liu et al. (2008, 2009) presented an ensemble-based four-dimensional variational (En4-DVar) algorithm, which uses the explicitly estimated **B**-matrix constructed by ensemble forecasts and performs 4-DVar optimization. Zhang et al. (2009) coupled 4-DVar with EnKF to produce a superior hybrid approach for

*Corresponding author: LASG, Institute of Atmospheric Physics, Beijing 100029, China.
e-mail: wab@lasg.iap.ac.cn
DOI: 10.1111/j.1600-0870.2010.00487.x

data assimilation (E4-DVar), which benefited from using the state-dependent uncertainty provided by EnKF while taking advantage of 4-DVar in preventing filter divergence. Every small step forward is the main booster of the improvements that have been made in data assimilation techniques and the scope of this paper is not to review all of the developments. Based upon the similar opinion, Wang et al. (2010) formulated a dimension-reduced projection 4-DVar (DRP-4-DVar) method, which directly obtained an optimal solution in the reduced space by fitting observations with ensemble and did not require implementation of tangent linear and adjoint models. The DRP-4-DVar approach contained some advantages. It presented a strong constraint with model, utilized all types of observations and made **B**-matrix more generally flow-dependent like EnKF. In theoretical aspect, Wang et al. (2010) had constructed the Observing System Simulation Experiments (OSSE) to evaluate the performance of DRP-4-DVar. They tested the method with a highly complex regional model and assimilating accumulated rainfall observations. In this paper, we will give a much more extensive analysis through a much simpler numerical model. Following the methodology of Zhang et al. (2009), Fertig et al. (2007) and Hunt et al. (2004), we conduct experiments using Lorenz-96 model. The results based on this model with a similar experimental setup will also allow the readers to compare the performance of DRP-4-DVar with other similar methods that have already been proposed in the literature.

A brief introduction of DRP-4-DVar and experimental design are presented in Sections 2 and 3, respectively. It is followed by OSSEs for various aspects of DRP-4-DVar in Section 4. Finally, a summary and conclusion are provided in Section 5.

2. A brief introduction of DRP-4-DVar

DRP-4-DVar algorithm has been presented in Wang et al. (2010). The approach directly obtains an optimal solution in the reduced space by fitting the observations with samples. The linearity assumption and the construction of **B** matrix are very important for DRP-4-DVar. From eq. 10 of Wang et al. (2010), the derivation of the proposed method explicitly depends on the fact that normalized observation increment simulation $\tilde{\mathbf{y}}'$ are linearly related to model initial increment $\mathbf{x}'$,

$$\begin{aligned}\tilde{\mathbf{y}}' &= \tilde{\mathbf{y}}'(\mathbf{x}') = \mathbf{R}^{-1}[\mathbf{H}(\mathbf{M}(\mathbf{x}_\mathrm{b}+\mathbf{x}',\tau)) - \mathbf{H}(\mathbf{M}(\mathbf{x}_\mathrm{b},\tau))] \\ &\approx \mathbf{L}_{(\mathbf{x}_\mathrm{b},\tau,\mathbf{R})}\mathbf{x}', \end{aligned} \tag{1}$$

where **H**, **M** and **L**, respectively represent the observation operator, prediction model and linear operator that is composed of the tangent linear model of **M** and tangent linear operator of **H**. The subscript $(\mathbf{x}_\mathrm{b},\tau,\mathbf{R})$ of **L** means **L** is with respect to the background field $\mathbf{x}_\mathrm{b}$, the time step τ and the observation error standard deviation **R**. This linear correspondence thus becomes a critical assumption in the validity of its solution. In order to give a detailed discussion of this fact and some quantitative analysis, we will design an experiment to test the impact of tangent linear approximation in this paper.

Wang et al. (2010) used the initial perturbation samples generated at the first step to estimate **B**-matrix explicitly,

$$\begin{cases} \mathbf{B} \approx \mathbf{b}\,\mathbf{b}^T \\ \mathbf{b} = \frac{1}{\sqrt{m-1}}(\mathbf{x}'_1 - \bar{\mathbf{x}}', \mathbf{x}'_2 - \bar{\mathbf{x}}', \cdots, \mathbf{x}'_m - \bar{\mathbf{x}}') \\ \bar{\mathbf{x}}' = \frac{1}{m}(\mathbf{x}'_1 + \mathbf{x}'_2 + \cdots + \mathbf{x}'_m) \end{cases} . \tag{2}$$

Here, the superscript T denotes the transpose. After it is projected from the control variable space onto the m-dimension sample space, it becomes a low-dimensional, constant matrix,

$$\mathbf{b}_\alpha = \frac{1}{\sqrt{m-1}} \begin{pmatrix} 1-\frac{1}{m} & -\frac{1}{m} & \cdots & -\frac{1}{m} \\ -\frac{1}{m} & 1-\frac{1}{m} & \cdots & -\frac{1}{m} \\ \vdots & \vdots & \ddots & \vdots \\ -\frac{1}{m} & -\frac{1}{m} & \cdots & 1-\frac{1}{m} \end{pmatrix}_{m\times m} . \tag{3}$$

The relationship between matrices **b** and $\mathbf{b}_\alpha$ is $\mathbf{b} = \mathbf{P}_x\mathbf{b}_\alpha$, where $\mathbf{P}_x$ is the projection matrix. However, this ensemble-based **B** matrix is not of full rank. Therefore, Wang et al. (2010) proposed a special inflation technique to overcome its singularity,

$$\mathbf{b}_\alpha = \frac{1}{\sqrt{m}} \begin{pmatrix} 1-\frac{1}{m+1} & -\frac{1}{m+1} & \cdots & -\frac{1}{m+1} \\ -\frac{1}{m+1} & 1-\frac{1}{m+1} & \cdots & -\frac{1}{m+1} \\ \vdots & \vdots & \ddots & \vdots \\ -\frac{1}{m+1} & -\frac{1}{m+1} & \cdots & 1-\frac{1}{m+1} \end{pmatrix}_{m\times m} . \tag{4}$$

As for the technique, we also design an experiment to test its impact.

3. Experimental design

An OSSE is considered as one of the best choices to assess data assimilation technique effectively. Here, to illustrate the implementation of four-dimensional assimilation of observations in the DRP-4-DVar, we design OSSEs using the Lorenz-96 model (Lorenz, 1996),

$$\frac{dx_j}{dt} = (x_{j+1} - x_{j-2})x_{j-1} - x_j + F, \tag{5}$$

where $j = 1, \ldots, M$ represents the spatial coordinate. Similar to atmospheric systems, the model has non-linear advection and sensitivity to initial conditions (ICs) and external forcing; this model can be thought of as disturbance propagation from West to East (Lorenz and Emanuel, 1998). In order to compare the performance of the DRP-4-DVar with that of traditional data assimilation methods (e.g. the standard 4-DVar and EnKF), an experiment setup similar to the one in the literatures (e.g. Hunt et al., 2004; Fertig et al., 2007; Khare et al., 2008; Zhang et al., 2009) is adopted. Here, the forcing parameter and the number of spatial elements are set to be $F = 8$ and $M = 40$, respectively. The model solves eq. (5) using a fourth-order Runge-Kutta scheme with a time stepping of 0.05 time unit, where

the boundary conditions of eq. (5) are periodic: $x_{j+m} = x_j$ and the 0.05 time unit is thought of as 6 h (Lorenz and Emanuel, 1998). Simulations during a period of time unit after a long-term integration (e.g. 10^5 model time steps) of the model from an arbitrary IC are assumed to be the 'true' states. Observation data sets include observations of all model variables that are produced by adding uncorrelated random noise with standard Gaussian distribution (with zero mean and variance of 0.16) to the true states every 6 h.

In the case $F = 8$ and $M = 40$, Zhang et al. (2009) showed the performance of the standard 4-DVar, EnKF and two coupled approaches in the top panel of Fig. 2 of their paper, from which we can easily find that the EnKF has a performance generally better than or at least comparable to the standard 4-DVar in the long assimilation cycles due to its flow-dependent **B**-matrix. For this reason, we hope to compare the performance of the DRP-4-DVar with that of the EnKF.

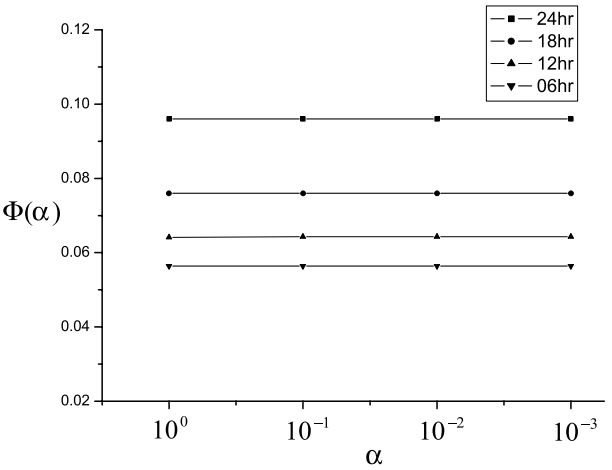

Fig. 1. The values of $\Phi(\alpha)$with respect to different α (10^0, 10^{-1}, 10^{-2} and 10^{-3}) in different time windows (6 h, 12 h, 18 h and 24 h).

4. Results

4.1. *Linearity check*

As mentioned above, the linear assumption is critical for DRP-4-DVar. Therefore, it is necessary to design an experiment to examine its impact on non-linear integration. In the DRP-4-DVar, the tangent linear approximation means

$$\mathbf{H}_i\{\mathbf{M}_{t_0\to t_i}[\mathbf{x}_g(t_0)+\delta\mathbf{x}(t_0)]\}-\mathbf{H}_i\{\mathbf{M}_{t_0\to t_i}[\mathbf{x}_g(t_0)]\}\approx\mathbf{L}_i\delta\mathbf{x}(t_0), \tag{6}$$

where $\mathbf{L}_i = \mathbf{H}'_i\mathbf{M}'_{t_0\to t_i}$. Set $\delta\mathbf{x}(t_0) = \alpha\delta\mathbf{x}_a(t_0)$ in which α is a small real number (e.g. $\alpha \leq 1$), then

$$\begin{aligned}&\mathbf{H}_i\{\mathbf{M}_{t_0\to t_i}[\mathbf{x}_g(t_0)+\alpha\delta\mathbf{x}_a(t_0)]\}-\mathbf{H}_i\{\mathbf{M}_{t_0\to t_i}[\mathbf{x}_g(t_0)]\}\\&\quad\approx\alpha\mathbf{L}_i\delta\mathbf{x}_a(t_0)\end{aligned} \tag{7}$$

and thus

$$\begin{aligned}\Phi(\alpha)&=\frac{\left\|\mathbf{H}_i\{\mathbf{M}_{t_0\to t_i}[\mathbf{x}_g(t_0)+\alpha\delta\mathbf{x}_a(t_0)]\}-\mathbf{H}_i\{\mathbf{M}_{t_0\to t_i}[\mathbf{x}_g(t_0)]\}\right\|}{\alpha}\\&\approx\left\|\mathbf{L}_i\delta\mathbf{x}_a(t_0)\right\|.\end{aligned} \tag{8}$$

It means that if the real function $\Phi(\alpha)$ keeps constant approximately when α is set to be different but small values, then the impact of the tangent linear approximation will be negligible. In fact, we use four different time windows, whose length t_i–t_0 is 6 h, 12 h, 18 h and 24 h, respectively, to calculate the values of $\Phi(\alpha)$ with respect to different α that is 1.0, 10^{-1}, 10^{-2} and 10^{-3}, respectively (marked 'EXP-1'). The results show that the values of $\Phi(\alpha)$ almost keep constant in the four windows (see Fig. 1). The shorter the window length is, the less impact the tangent linear approximation has. It indicates that the linearity assumption was feasible and reasonable for a 24-h or shorter assimilation window in the Lorenz-96 model.

As for the impact of the tangent linear approximation on the 4-DVar implementation based on a complex full-physics forecast model, Guo et al. (2000) concluded that, in the rainfall data assimilations using the 4-DVar system of the fifth-generation Pennsylvania State University-National Centre for Atmospheric Research Mesoscale Model (MM5), a 3-h and a 6-h time windows work equally well and the 3-h window has the advantage of saving the space for storing the basic state trajectories. However, a 12-h time window leads to an unsuccessful minimization. Therefore, the length of the assimilation window in 4-DVar should be long enough to ensure fully developed dynamic structure functions, but should be shorter than the limitation constrained by the assumption of perfect model and the validity of tangent-linear hypothesis. Some experiments of DRP-4-DVar in Wang et al. (2010) with MM5 also showed that it worked well for 3 h or 6 h time windows.

4.2. *DRP equivalence*

We design an experiment (marked 'EXP-2') to examine the equivalence between the EnKF and the DRP-4-DVar when the assimilation window of the DRP-4-DVar is degenerated to only include analysis time (i.e. the DRP-4-DVar is used as a 3-DVar with a flow-dependent **B**-matrix, without the dimension in time).

In this case, both approaches assimilate the same observations at each analysis time and use the same ensemble size that is set to be 500 and their results are compared with the same 'true' states. The ensemble size is large enough so that the correlations between two different variables in the **B**-matrix have high significance level and no localization is needed, but the covariance inflation method of Zhang et al. (2009) was used in this experiment:

$$(x'_i)_{new} = \alpha(x'_i)^f + (1-\alpha)(x'_i)^a, \tag{9}$$

where α is the relaxation coefficient, $(x'_i)^f$ and $(x'_i)^a$ denote the prior (forecast) and the posterior (analysis) perturbations,

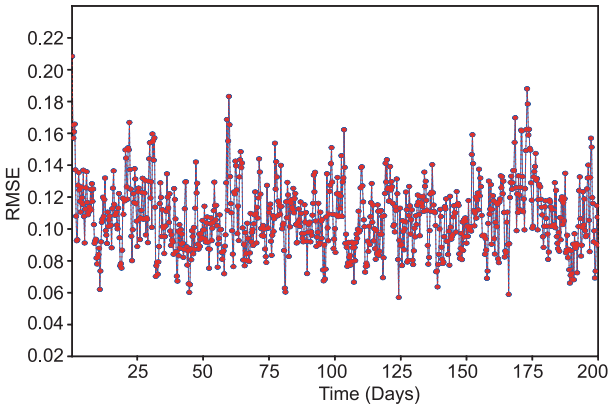

Fig. 2. RMSEs of the analysis by the EnKF (red curve with dots) and the sequential DRP-4-DVar (blue curve with circles) during 200 days.

respectively. And $(x_i')_{new}$ is the final perturbation of the analysis ensemble used for the next forecast cycle. In this experiment, $\alpha = 0.15$ is used.

Here, DRP-4-DVar uses the singular $\mathbf{b}_\alpha$ determined by eq. (3) for estimating the **B**-matrix by eq. (2) to ensure the equivalence between both approaches in theory. Over a period of 40 time units, we assimilate the observations once every 6 h (i.e. 0.05 time unit) using the DRP-4-DVar and EnKF. It takes 800 steps to complete this long-term assimilation cycle.

Figure 2 shows the root mean square errors (RMSEs) of the analysis from two approaches (red curve with dots for the EnKF and blue curve with circles for the DRP-4-DVar) at each step. The RMSEs in the DRP-4-DVar analysis are exactly equal to those in the EnKF analysis (Fig. 1). The results demonstrate that the DRP-4-DVar has the same performance as the EnKF when it is used as a 3-DVar that excludes the time dimension.

4.3. *Impact of assimilation window*

When a time dimension is included as it is originally designed, the DRP-4-DVar is a 4-DVar with a flow-dependent **B**-matrix. In this case, it is theoretically anticipated to outperform both the standard 4-DVar and EnKF, because it has a better **B**-matrix than the standard 4-DVar and is more consistent with forecast model than the EnKF due to the inclusion of dynamical and physical constraints in its analysis through the time dimension at each analysis time. To test this theoretical anticipation, we conduct an assimilation experiment (named 'EXP-3') over a period of 200 days using the DRP-4-DVar with 18-h assimilation window. The estimation of the **B**-matrix for the DRP-4-DVar, the ensemble size, the covariance inflation, the observations for assimilations and the 'true' states for comparisons during this period in this experiment are the same as in EXP-2. The difference is that EXP-2 only assimilates synchronous observations at analysis time at each assimilation cycle, while this experiment assimilates observations at four different times, including the analysis time and 6 h, 12 h and 18 h after the analysis time at each cycle.

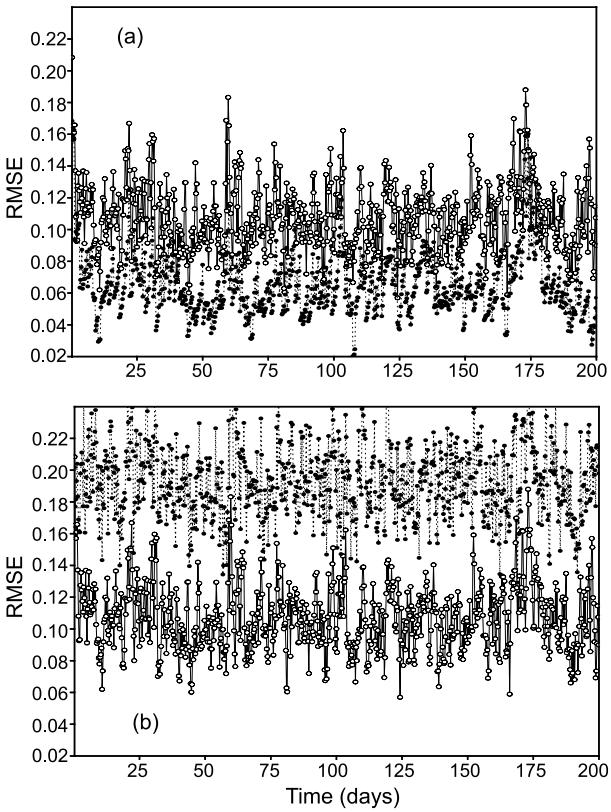

Fig. 3. (a) RMSEs of the analysis by the DRP-3-DVar (solid curve with circles) and the DRP-4-DVar (dashed curve with dots) during 200 days, (b) RMSEs of the analysis by the DRP-3-DVar (solid curve with circles) and standard 3-DVar (dashed curve with dots) during 200 days.

It implements assimilation cycle every 24 h to avoid the repeating use of the observations and takes 200 steps to complete all the assimilation cycles over the same period. In order to conveniently compare the accuracies of analysis from both experiments, the RMSEs of analysis in this experiment are calculated every 6 h through comparing the analysis and the 6-h, 12-h and 18-h forecasts initialized by the analysis with the corresponding 'true' states. Figure 3a gives the comparison of RMSEs between the two experiments, in which the dashed curve with dots represent the RMSEs from the DRP_4-DVar with 18-h assimilation windows in a non-sequential manner in this experiment and the solid curve with circles mark are those from the DRP-4-DVar used as a 3-DVar in a sequential way in the previous experiment with a 6-h cycle. Obviously, better performance from the non-sequential approach can be observed. Comparing with the sequential method, it produces more accurate analysis. It means that the non-sequential DRP-4-DVar outperforms the EnKF according to the equivalence between the EnKF and the sequential DRP-4-DVar. It maybe also performs better than the standard

4-DVar because the top panel in Fig. 2 of Zhang et al. (2009) showed the performance of the EnKF was generally better or at least comparable to the standard 4-DVar. In addition, we also make comparison between the standard 3-DVar and DRP-3-DVar (Fig. 3b). Computing in the lower-dimension model is so fast that we really can't tell which method costs less. Figure 3b compares the performances of both DA methods. Obviously, the DRP-3DVar has less RMSE than the standard 3-DVar.

4.4. *Sensitivity to singularity and flow-dependence*

In order to alleviate the singularity as well as the underestimation of the **B**-matrix, Wang et al. (2010) proposed a non-singular $\mathbf{b}_\alpha$ on the ensemble space in eq. (4) for estimating **B**-matrix by $\mathbf{b} = \mathbf{P}_x\mathbf{b}_\alpha$ and the first expression in eq. (2). Here, we design an experiment (called 'EXP-4') to compare the performance of the non-singular $\mathbf{b}_\alpha$ determined by eq. (4) with that of the singular $\mathbf{b}_\alpha$ determined by eq. (3) in the DRP-4-DVar. Because the impact of the singularity of **B**-matrix on analysis will be more significant when the ensemble size is smaller, the size is reduced from 500 to 90 and the length of assimilation window is shortened from 18 h to 6 h in this experiment. In EXP-4, the covariance inflation is also included to avoid divergence. Figure 4 gives the differences between the RMSEs of analysis respectively with the non-singular and singular $\mathbf{b}_\alpha$ every 6 h during the 200 days. Negative value means a smaller RMSE of analysis with the non-singular $\mathbf{b}_\alpha$ than with the singular $\mathbf{b}_\alpha$. The curve is made with 800 values, among which 511 values are negative and the rest are positive. It indicates that more than 74% of analyses with the non-singular $\mathbf{b}_\alpha$ have smaller RMSEs. Especially, significant improvement of analysis by the non-singular $\mathbf{b}_\alpha$ can be observed during the last 25 days before the divergence occurs.

At last, we design an experiment (named 'EXP-5') to investigate the role of flow-dependence of **B**-matrix in the DRP-4-DVar. There are two kinds of flow-dependence in **B**-matrix. One is explicitly estimated or the flow of the day (Hamill et al., 2002),

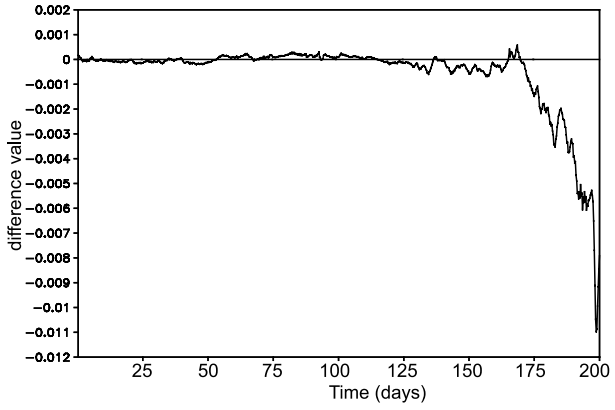

Fig. 4. Differences between the RMSEs of analysis by the DRP-4-DVar with the non-singular and singular $\mathbf{b}_m^\alpha$, respectively, where negative value means smaller RMSEs with the non-singular $\mathbf{b}_m^\alpha$.

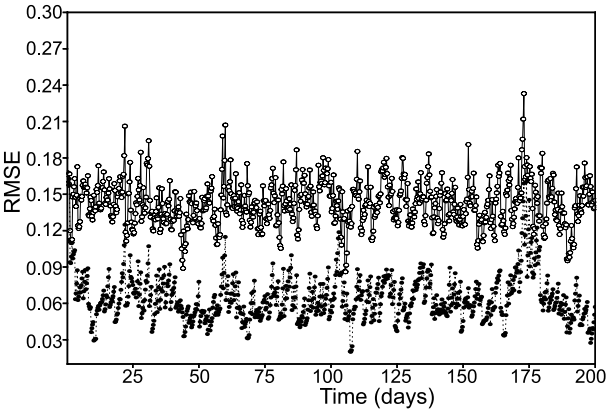

Fig. 5. RMSEs of analysis by the DRP-4-DVar with explicitly flow-dependent (dashed curve with dots) and implicitly flow-dependent (solid curve with circles) **B**-matrices.

which means the **B**-matrix keeps developing from one cycle of assimilation to another. The other is implicitly estimated, which means the **B**-matrix is fixed or static at each cycle, varies with the states inside the assimilation window but does not evolve to the next cycle. For example, the **B**-matrix used in the EnKF has the feature of explicit flow-dependence, but it is not implicitly developed because of the absence of time dimension at each cycle. The standard 4-DVar uses an implicitly estimated **B**-matrix. The DRP-4-DVar uses a **B**-matrix with both explicit and implicit estimates, because at each cycle it is an incremental 4-DVar and from one cycle to another the ensemble samples used for estimation of **B**-matrix vary with the flow. This is the reason why the DRP-4-DVar outperforms both the EnkF and standard 4-DVar. In this experiment, two kinds of **B**-matrices are used in the DRP-4-DVar. One is estimated with random perturbation samples at every cycle of assimilation. The other is estimated with random perturbation samples only at the first cycle and with the analysed samples at other cycles. When both **B**-matrices are used in the DRP-4-DVar with 18-h assimilation windows in this experiment, they are implicitly and explicitly estimated, respectively. The results show that the DRP-4-DVar with the explicitly estimated **B-**matrix produces smaller RMSEs of analysis than it does with the implicitly estimated **B-**matrix (see Fig. 5). It again demonstrates the important role of the explicitly estimated **B**-matrix in a 4-DVar approach.

5. Summary and conclusions

In this paper, we evaluate the DRP-4-DVar based on the Lorenz-96 perfect model. Two idealized experiments (EXP-2 and EXP-3) are conducted, which provide a proper framework for assessing the performance of this new method. If only the synchronous observations at analysis time are sequentially assimilated like a 3-DVar approach in EXP-2, the DRP-4-DVar is exactly equivalent to the EnKF. When it is used as a non-sequential approach as it is originally designed in EXP-3, the new method produces better analysis than the EnKF does. The significant

amelioration by the new approach results from both the consistency that the DRP-4-Dvar takes the model as the most appropriate constraint and the use of explicit flow-dependent **B**-matrix.

Intrinsic non-linearity in the laws governing the atmospheric flow limits the use of the tangent linear approximation. Therefore, it is necessary to make sure for what a length of assimilation window this approximation is feasible and reasonable. For a 24-h or shorter assimilation window, the impact of linearity assumption is proven to be negligible in EXP-1 using the Lorenz-96 model. For a more realistic implementation of 4-DVar using a complex full-physics forecast model, the length of the assimilation window should be long enough to ensure fully developed dynamic structure functions, but should be shorter than the limitation constrained by the assumption of perfect model and the validity of tangent-linear hypothesis.

EXP-4 further shows that with the **B**-matrix having the non-singular projection onto the ensemble space, the DRP-4-DVar yields a better performance than it does with the **B**-matrix using the singular projection onto the ensemble space. Meanwhile, EXP-5 demonstrates the important role of explicitly estimated **B-**matrix in the DRP-4-DVar. The possession of the features of both explicit and implicit estimates in the new approach is the main reason why it outperforms both the EnKF and the standard 4-DVar.

When an imperfect model is used, Zhang et al. (2009) found the standard 4-DVar may have an unacceptable RMSE and the standard EnKF even do not converge, but the couple approach can achieve an acceptable performance. Another work finished (Zhao et al., 2010) by our research group also shows that the DRP-4-DVar with imperfect model performs well, similar to the couple approach of Zhang et al. (2009), which will be introduced in details in the other paper.

In real applications, the model state and the observation vector generally have high dimensions (say 10^6 and 10^4, respectively), how to improve the quality of the ensemble is a key problem. Moreover, the ensemble size dimension is much lower (e.g. 10^2), in this case, localization is needed to ameliorate the singularity of B-matrix and to filter some spurious long-range correlations in it.

6. Acknowledgments

We acknowledge the China Meteorological Administration for the R&D Special Fund for Public Welfare Industry (meteorology) (Grant No. GYHY(QX)200906009), the National High Technology Research and Development Program of China (863 Program, No. 2010AA012304) and the LASG free exploration fund.

References

Buehner, M. 2005. Ensemble-derived stationary and flow-dependent background error covariances: evaluation in a quasi-operational setting for NWP setting. *Quart. J. Roy. Meteor. Soc.* **131**, 1013–1043.

Caya, A., Sun, J. and Snyder, C. 2005. A comparison between the 4DVAR and the ensemble Kalman filter techniques for radar data assimilation. *Mon. Wea. Rev.* **133**, 3081–3094.

Courtier, P., Thépaut, J.-N. and Hollingsworth, A. 1994. A strategy for operational implementation of 4D-Var using an incremental approach. *Quart. J. Roy. Meteor. Soc.* **120**, 1367–1387.

Courtier, P. and Talagrand, O. 1987. Variational assimilation of meteorological observations with the adjoint vorticity equation. II: numerical results. *Quart. J. Roy. Meteor. Soc.* **113**, 1329–1347.

Evensen, G. 1994. Sequential data assimilation with a nonlinear quasi-geostrophic model using Monte Carlo methods to forecast error statistics. *J. geophys. Res.* **99**(C5), 10143–10162.

Evensen, G. and van Leeuwen, P. J. 2000. An ensemble Kalman smoother for nonlinear dynamics. *Mon. Wea. Rev.* **128**, 1852–1867.

Fertig, E., Harlim J. and Hunt, B. 2007. A comparative study of 4D-Var and 4D. Ensemble Kalman Filter: perfect model simulations with Lorenz-96. *Tellus* **59A**, 96–100.

Gustafsson, N. 2007. Discussion on '4D-Var or EnKF?' *Tellus* **59A**, 774–777.

Guo, Y.-R., Kuo, Y.-H., Dudhia, J., Parsons, D. and Rocken, C. 2000. Four-dimensional variational data assimilation of heterogeneous mesoscale observations for a strong convective case. *Mon. Wea. Rev.* **128**, 619–643.

Hamill, T. M. and Snyder, C. 2000. A hybrid ensemble Kalman filter—3D variational analysis scheme. *Mon. Wea. Rev.* **128**, 2905–2919.

Hamill, T. M., Snyder, C. and Morss, R. E. 2002. Analysis-error statistics of a quasi-geostrophic model using 3-dimensional variational assimilation. *Mon Wea. Rev.* **130**, 2777–2790.

Houtekamer, P. L. and Mitchell, H. L. 1998. Data assimilation using an ensemble Kalman filter technique. *Mon. Wea. Rev.* **126**, 796–811.

Houtekamer, P. L. and Mitchell, H. L. 2001. A sequential ensemble Kalman filter for atmospheric data assimilation. *Mon. Wea. Rev.* **129**, 123–137.

Hunt, B. R., Kalnay, E., Kostelich, E. J., Ott, E., Patil, D. J. and co-authors. 2004. Four-dimensional ensemble Kalman filtering. *Tellus* **56A**, 273–277.

Kalnay, E., Li, H., Miyoshi, T., Yang, S.-C. and Ballabrera-Poy, J. 2007a. 4D-Var or ensemble Kalman filter? *Tellus* **59A**, 758–773.

Kalnay, E., Li, H., Miyoshi, T., Yang, S.-C. and Ballabrera-Poy, J. 2007b. Response to the discussion on "4-D-Var or EnKF?" by Nils Gustafsson. *Tellus* **59A**, 778–780.

Khare, S. P., Anderson, J., Hoar, T. J. and Nychka, D. 2008. An investigation into the application of an ensemble Kalman smoother to high-dimensional geophysical systems. *Tellus* **60A**, 97–112.

Le Dimet, F.-X. and Talagrand, O. 1986. Variational algorithms for analysis and assimilation of meteorological observations: theoretical aspects. *Tellus* **38A**, 97–110.

Liu, C. S., Xiao, Q. and Wang, B. 2009. An Ensemble-based four-dimensional variational data assimilation scheme: part II: observing system simulation experiments with the Advanced Research WRF (ARW). *Mon. Wea. Rev.* **137**, 1687–1704.

Liu, C. S., Xiao, Q. and Wang, B. 2008. An Ensemble-based four-dimensional variational data assimilation scheme: part I: technical formulation and preliminary test. *Mon. Wea. Rev.* **136**, 3363–3373.

Lorenc, A. C. 2003. The potential of the ensemble Kalman filter for NWP—a comparison with 4D-VAR. *Quart. J. R. Meteorol. Soc.* **129**, 3183–3203.

Lorenz, E. and Emanuel, K. 1998. Optimal sites for supplementary weather observations: simulation with a small model. *J. Atmos. Sci.* **55**, 399–414.

Lorenz, E. 1996. Predictability: a problem partly solved. In: *Proc. Seminar on Predictability*. Volume 1, reading, ECMWF, United Kingdom, 1–19.

Rabier, F., Järvinen, J., Klinker, E., Mahfouf, J. F. and Simmons, A. 2000. The ECMWF implementation of four-dimensional variational assimilation. I: experimental results with simplified physics. *Quart. J. Roy. Meteor. Soc.* **126**, 1143–1170.

Rawlins, F., Ballard, S. P., Bovis, K. J., Clayton, A. M., Li, D. and co-authors. 2007. The Met Office global four-dimensional variational data assimilation scheme. *Quart. J. Roy. Meteor. Soc* **133**, 347–362.

Wang, B., Zou, X. and Zhu, J. 2000. Data assimilation and its application. *Proc. Natl. Acad. Sci. USA* **97**, 11143–11144.

Wang, B., Liu, J.-J., Wang, S., Cheng, W., Liu, J. and co-authors. 2010. An economical approach to four-dimensional variational data assimilation. *Adv. Atmos. Sci.* **27**, 715–727, doi:10.1007/s00376-009-9122-3.

Wang, X., Snyder, C. and Hamill, T. M. 2007. On the theoretical equivalence of differently proposed ensemble- 3DVAR hybrid analysis schemes. *Mon. Wea. Rev.* **135**, 222–227.

Xiao, Q.-N., Zou, X. and Wang, B. 2000. Initialization and simulation of a landfalling hurricane using a variational bogus data assimilation scheme. *Mon. Wea. Rev.* **128**, 2252–2269.

Yang, S. C., Corazza, M., Carrassi, A., Kalnay, E. and Miyoshi, T. 2009. Comparison of local ensemble transform Kalman filter, 3DVAR, and 4DVAR in a quasigeostrophic model. *Mon. Wea. Rev.* **137**, 693–709.

Zhang, F., Zhang, M. and Hansen, J. A. 2009. Coupling ensemble Kalman filter with four- dimensional variational data assimilation. *Adv. Atmos. Sci.* **26**, 1–8.

Zhao, J., Wang, B. and Liu, J.J. 2010. Impact of analysis-time tuning on the performance of DRP-4DVar approach. *Adv. Atmos. Sci.*, doi:10.1007/s00376-010-9191-3.

Zou, X., and Kuo, Y.-H. 1996. Rainfall assimilation through an optimal control of initial and boundary conditions in a limited-area mesoscale model. *Mon. Wea. Rev.* **124**, 2859–2882.